NUMERICAL SIMULATION OF CRUDE OIL-WATER FLOW PHASE SEPARATION IN T-JUNCTION

by

SITI HAJAR AISYAH BINTI MAT SOH

Dissertation submitted in partial fulfillment of
the requirements for the
Bachelor of Engineering (Hons)
(Petroleum Engineering)

SEPT 2013

Universiti Teknologi PETRONAS
Bandar Seri Iskandar
31750 Tronoh
Perak Darul Ridzuan

SITI HAJAR AISYAH BT. MAT SOH B. ENG (HONS) PETROLEUM ENGINEERING SEPT 2013

NUMERICAL SIMULATION OF CRUDE OIL-WATER FLOW PHASE SEPARATION IN T-JUNCTION

SITI HAJAR AISYAH BT. MAT SOH

PETROLEUM ENGINEERING

UNIVERSITI TEKNOLOGI PETRONAS

SEPT 2013

CERTIFICATION OF APPROVAL

NUMERICAL SIMULATION OF CRUDE OIL-WATER FLOW PHASE SEPARATION IN T-JUNCTION

by

Siti Hajar Aisyah Binti Mat Soh

A project dissertation submitted to the

Petroleum Engineering Programme

Universiti Teknologi PETRONAS

in partial fulfillment of the requirement for the

BACHELOR OF ENGINEERING (Hons)

(PETROLEUM ENGINEERING)

Approved by,

_____

Dr. William Pao King Soon

UNIVERSITI TEKNOLOGI PETRONAS

TRONOH, PERAK

SEPT 2013

CERTIFICATION OF ORIGINALITY

This is to certify that I am responsible for the work submitted in this project, that the original work is my own except as specified in the references and that the work contained herein have not been undertaken or done by unspecified sources or persons.

_____

SITI HAJAR AISYAH BINTI MAT SOH

ABSTRACT

T-junctions are very common within pipe networks in a wide range of industrial applications in the chemical and petroleum industries. Understanding the behavior of liquid-liquid two-phase flow through a T-junction is very important as it has significant effect on the operation, maintenance and efficiency of the components downstream from the junction. Specifically this project objectives are i) to investigate the geometric effect on separation efficiency in T-junction, and ii) to analyze the fraction of oil taken off in a T-junction at different operating conditions and parameters. The phase distribution of the two-phase flow is simulated using FLUENT. The diameter ratio, length ratio, inlet oil fraction, density ratio and mixture velocity ratio are identified as the main factors affecting the fraction of oil taken off in T-junction. At the end of this project, it is observed that the density ratio plays the most important role on phase separation, followed by mixture velocity ratio and length ratio. Conversely, both diameter ratio and inlet oil fraction have least impact on phase separation efficiency. The efficiency of phase separation and the geometric effect of the T-junctions on the flow split are understood in order to achieve an optimum passive separation performance for optimal operation of downstream components from the junction.

Table of Contents

ABSTRACT ..... **i**

LIST OF FIGURES ..... **iv**

LIST OF TABLES ..... **vi**

CHAPTER 1: INTRODUCTION **1**

1.1 Project Background 1
1.2 Problem Statement 2
1.3 Objective 2
1.4 Scope of Study 3
1.5 Relevancy of Project 3
1.6 Feasibility of Project 3

CHAPTER 2: LITERATURE REVIEW **4**

2.1 Flow patterns 4
2.2 Introducing Junctions and Liquid-liquid Phase Flow 7
2.3 The Flow Map 9
2.4 The Simple T-junction ..... .10
2.5 Separation Efficiency……....11
2.6 Ideal Separation ..... .13

CHAPTER 3: METHODOLOGY **14**

3.1 Development of Model Simulation 14
3.2 Mesh dependency check analysis 18
3.3 Project methodology and activities 21

3.4 Gantt Chart and Key Milestone for FYP I 22
3.5 Gantt Chart and Key Milestone for FYP II 23
3.6 Tools required 24

CHAPTER 4: RESULTS & DISCUSSIONS 25

4.1 Verification of the simulation model with experiment data 25
4.2 Parametric Studies on Two-Phase separation Efficiency in T-junction... 28
4.3 Concluding Remarks 37

CHAPTER 5: CONCLUSSIONS & RECOMMENDATION 40

REFERENCES 42

LIST OF FIGURES

Figure 1.1	Diagram of a T-junction	1
Figure 2.1	Oil water flow patterns in vertical pipes	5
Figure 2.2	Oil water flow patterns in horizontal pipes	7
Figure 2.3	Generic Flow Map for Horizontal Flow	8
Figure 2.4	General Flow Map for Vertical Flow	8
Figure 2.5	Parameters of two-phase flow at T-junction	11
Figure 2.6	Separation efficiency derived from the traditional expression for separation results of a T-junction	12
Figure 3.1	Schematic T-Junction with applied inlet and outlet boundary conditions	17
Figure 3.2	Graph of pressure versus mesh density	18
Figure 3.3	Computational mesh refinement of T-junction	19
Figure 3.4	Pressure contour of mixture phase with total number of 25128 and 160099 tetrahedral cells respectively	19
Figure 3.5	Velocity contour of water phase with total number of 25128 and 160099 tetrahedral cells respectively	20
Figure 3.6	Velocity contour of oil phase with total number of 25128 and 160099 tetrahedral cells respectively	20
Figure 3.7	Four phases of project methodology and activities	21
Figure 4.1	Computational grid of T-junction	26
Figure 4.2	Simulated flow split curves compared with experimental results	27
Figure 4.3	Effect of diameter ratio on fraction of oil taken off with initial velocity of 0.4m/s and pentane density of 626kg/m^3	28
Figure 4.4	Effect of inlet oil fraction on fraction of oil taken off with initial mixture velocity of 0.4m/s and oil density of 626kg/m^3	30

Figure 4.5	Effect of length ratio on oil taken off with initial mixture velocity of 0.4m/s and oil density of 626kg/m^3	32
Figure 4.6	Effect of mixture velocity ratio on oil taken off at density ratio of 0.70 and 0.90, and length ratio of 0.50 and 0.70 for mass split ratio, M of 0.30 and 0.70	34
Figure 4.7	Effect of density ratio on oil taken off at inlet oil ratio of 0.30 and 0.80, and diameter ratio of 0.50 and 1.00	35
Figure 4.8	Parameters' weighting factor on two-phase separation in T-junction	38
Figure 4.9	Parameters' sensitivity to fraction of oil taken off	38
Figure 4.10	Parameters' weighting factor based on percentage	39

LIST OF TABLES

Table 3.1	Input parameters for validation and parametric studies	17
Table 3.2	Gantt chart and key milestone for FYP I	22
Table 3.3	Gantt chart and key milestone for FYP II	25
Table 4.1	Fraction of oil taken off per unit change of diameter ratio for mass split ratio, M of 0.20, 0.40, 0.60 and 0.80	29
Table 4.2	Fraction of oil taken off per unit change of inlet oil fraction for mass split ratio, M of 0.20, 0.40, 0.60 and 0.80	31
Table 4.3	Fraction of oil taken off per unit change of length ratio for mass split ratio, M of 0.20, 0.40, 0.60 and 0.80	33
Table 4.4	Fraction of oil taken off per unit change of velocity ratio with variation of density ratio and diameter ratio	34
Table 4.5	Fraction of oil taken off per unit change of density ratio with variation of inlet oil fraction and diameter ratio	36

CHAPTER 1

INTRODUCTION

1.1 Project Background

Two-phase flow is a simultaneous flow of two immiscible fluids, which are often found in a wide range of industrial applications in the chemical and petroleum industries. For instance, gas-liquid two-phase flows occur in distillation, absorption and evaporation; liquid-liquid two-phase flows in extraction; and various two-phase flows in heterogeneous chemical reaction in the petrochemical industry. Basically, there are four categories of two-phase flow; gas-liquid, gas-solid, liquid-liquid and liquid-solid flows. Among these two-phase flow, there are particular concern in the flows in the oil production industry where crude oil mixed with natural gas, water and frequently sand. For the sake of economic and safety reason, each of these components needs to be separated out before being transported to their destination.

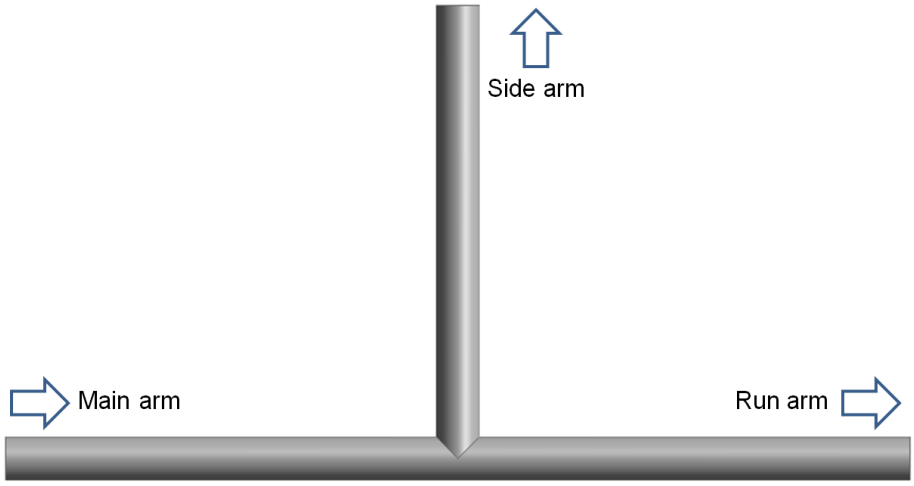

Figure 1.1 Diagram of a T-junction (Wang *et al*., 2007)

A T-junction or known as ‘T’ pipe is a common component in pipe network, mainly involve in mixing and splitting the fluids. It consists of three main parts which are main arm, branch arm and run arm. When two-phase flow encounters a T-junction, the uneven phase distribution would occur between the outlets which are run and branch arm. Numerous experiments conducted to study this phenomenon reported that the factors affecting the split flow including an under-pressure in the branch, the mass inertia of the liquid, the flow pattern upstream and the geometry of the T-junction itself.

1.2 Problem Statement

T-junction as an efficient partial phase separator can significantly reduce the processing load on the main separator. However, the major efforts in the study of phase separation through T-junctions have been limited only to gas-liquid flows. Although the accurate prediction of liquid-liquid especially oil-water flow is essential, this flow behavior in pipes has not been explored much. Knowledge of the distinctive features of oil-water mixtures together with those gas-liquid systems can be used in the future as a basis to understand the more complex case of gas-oil-water flow.

1.3 Objectives

The objectives of this project are:

a) To investigate the geometric effect on separation efficiency in T-junction
b) To analyze the fraction of oil taken off in a T-junction at different operating conditions and parameters

1.4 Scope of Study

The main focus of the project is to investigate the effect of upstream flow pattern on the flow split and as well as to study the influence of varying the diameter ratio of side arm to main arm in T-junction. Besides that, the effect inlet flow condition under constant pressure will be investigated with the scope of circular cross sectional area of T-junction, horizontal main arm and vertical side arm by using crude oil and water as working fluids.

1.5 Relevancy of the Project

This project is relevant to the author's field of majoring since the study of oil and water two-phase flow in a natural environment is one of the focus areas in drilling process. Meanwhile the designing of a separation in pipeline system, this project provides more understanding on the flow characteristics of the fluids, making the parameters for modeling process easier and targeted are known.

1.6 Feasibility of the Project

Within the given time frame, it is feasible to complete the project while maintaining a consistency throughout the project.

During the first part of the project (FYP I), the scope of work for the project will be:

a) Research on the flow characteristics of the oil and water phase and the models to be used for the simulation
b) Progress reporting to supervisor to ensure the study still on the right track
c) Familiarization with the software that will be used during simulation process

During the second part (FYP II), the scope of work will be:

a) Performing the simulation of the project
b) Improving and analyzing the simulation
c) Preparing the academic paper

CHAPTER 2

LITERATURE REVIEW

2.1 Flow Patterns

There are two main types of flow in pipes which are vertical flow and horizontal flow.

2.1.1 Vertical flow in pipes

Abduvayt *et al*. (2006) and Flore *et al*. (1999) stated that oil-water flows distribute themselves into six main patterns and group into two categories as oil-dominated and water-dominated flow in vertical pipes.

Water-Dominated Flow: In this flow, the water phase is continuous and the oil phase is in the form of droplets, dispersions, or chaotically large droplets as shown in the Figure 2.1.

- **Dispersion of oil in water**: Relatively large droplets of oil were carried in a continuous water phase that distributed over the entire pipe cross section at low oil and water flow rates. According to Abduvayt et al. (2006) when water-flow rate increased, various shapes of oil droplets could be observed ranging from large spherical droplets to small and medium sized globules.
- **Very fine dispersion of oil in water**: When the water-flow rate of dispersion of oil in water flow was increased, this flow pattern occurs with the appearance of oil in water emulsion that distributed almost evenly over entire pipe cross section.

- **Oil in water froth**: a highly turbulent flow pattern occurred at transitional region of oil dominated and water dominated regions affected by agglomeration and coalescence of large oil droplets and globules.

Oil-Dominated Flow: In this flow, the oil phase is continuous and the water phase is in the form of droplets, dispersions or chaotically large droplets as shown in Figure 2.1.

- **Dispersion of water in oil**: when the oil flow rate increased for water dominated flow with relatively low water flow rates, large water bodies would break into regularly shaped droplets and frequently flow over the entire pipe cross section.
- **Very fine dispersion of water in oil**: this flow occurred at relatively high flow rates of the oil phase characterized by a flow with very small water droplets distributed in a continuous, fast moving oil phase over the entire cross-sectional area of the pipe. This flow could be considered a homogeneous mixture.
- **Water in oil froth**: This flow pattern is known to be a very chaotic flow pattern. The water phase would flow as irregular large bodies and smaller droplets in the continuous oil phase with intermittently thin water film around the pipe wall.

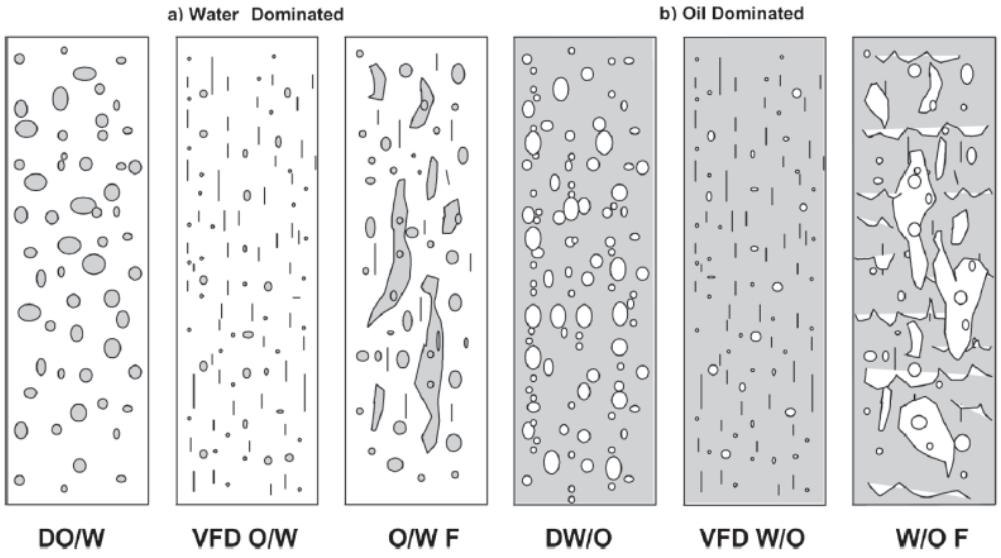

Figure 2.1 Oil-water flow patterns in vertical pipes (Abduvayt *et al*., 2006)

2.1.2 Horizontal flow in pipes

According to Trallero et al., (1997) there are six main categories of oil-water flow pattern in horizontal pipes as shown in the Figure 2.2.

- **Stratified smooth:** This flow pattern occurs at relatively low oil and water flow rates. The two phases are segregated by gravity with a smooth oil-water interface.
- **Stratified flow with mixing at the interface**: this flow pattern also known as stratified wavy flow. The form of flow pattern looks like stratified smooth flow however the waves formed on the interface are affected by the increased of velocity of either of the phase.
- **Dispersion of oil in water:** Water are occupied most of the cross section of the pipe and oil flowed at the top with varying widths of interface. This flow pattern occurs at relatively high water flow rates in horizontal pipe.
- **Oil in water emulsion:** When the oil flow rate of both phases are increased at oil dispersion in water flow, the oil-water interface become a roll wavy interface, while oil droplets in the water are lost and water droplets in oil are separated slightly from the interface.
- **Dispersion of water in oil and oil in water:** When the water flow rate is again increased slightly at stratified smooth flow, oil and water droplets are developed in the opposite phase and booth remains close to the interface. The oil droplet sizes are smaller than water droplet sizes.
- **Water in oil emulsion:** When the water flow rate is increased at oil dispersion in water flow, very small water droplets appears in oil while there is no dispersion of oil in water.

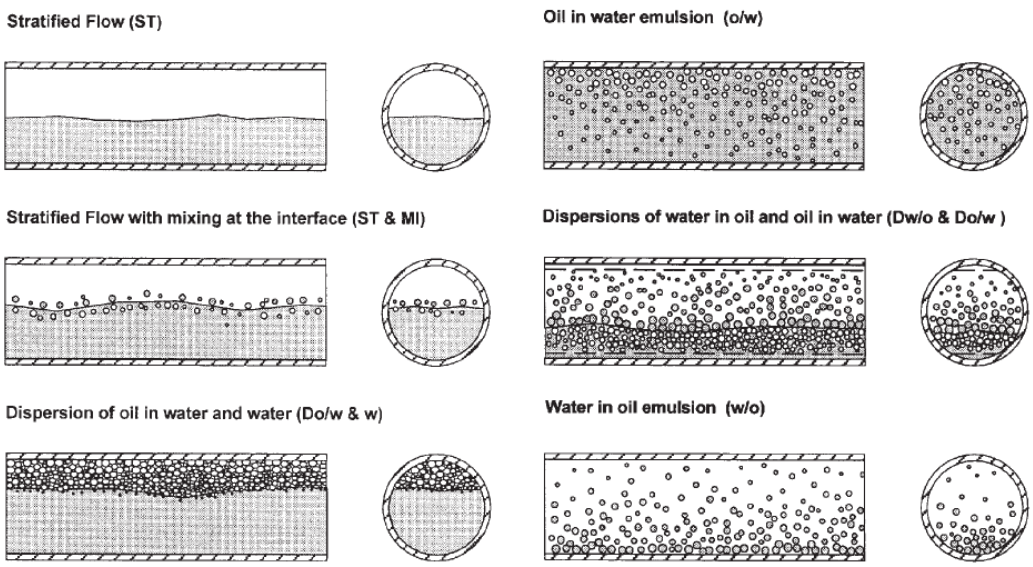

Figure 2.2 Oil-water flow patterns in horizontal flows (Trallero *et al*., 1997)

2.2 Flow Pattern Map

Among the factors that contribute to the variation of flow pattern are the dynamic and hydrodynamic effects, geometric distribution or topography of the flow lines or pipelines and volumetric or mass flow rates of each of the phases. All these parameters present a major challenge to determine the transition boundaries as most of the flow regime determination are done in laboratory through visual observations and dependent on the observer's interpretation.

Studies on flow pattern and its transition behaviour have been conducted through visual observation in a transparent pipe. Data from these experiments have been mapped on a two dimensional plot to determine the boundaries of all the studied flow patterns for empirical correlation development purposes. The published experimental flow patterns studies used a selection of mapping coordinates such as the mass flow rates as used by Bergelin and Gazley (1949) and Abou- Sabe Johnson (1952) or the superficial velocities as used by Alves (1954).

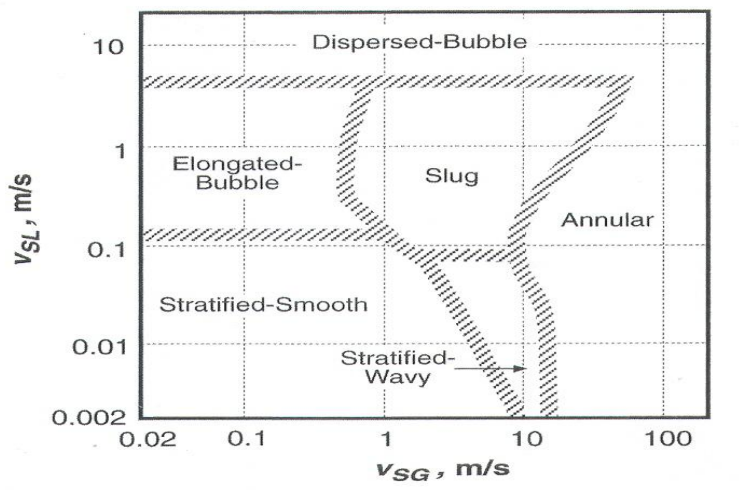

Figure 2.3 Generic flow map for horizontal flow (Mandhane, 1984)

However, the classification of the flow regime map can be categorized in either horizontal or vertical flow regimes. For horizontal flow, flow pattern and the transitions behaviour are dependent of the pipe diameter, fluid properties of the phases and the superficial gas and liquid velocities. This flow map is represented in terms of superficial liquid and gas velocity, V_{SL} and V_{SG} respectively. A generic flow map for horizontal flow is shown in Figure 2.3. In vertical flow, the stratified flow regime disappeared and a new pattern is observed, namely Churn Flow. Normally the flow patterns in vertical flow are more symmetric around the pipe axis. A generic flow map for vertical flow is shown in Figure 2.4.

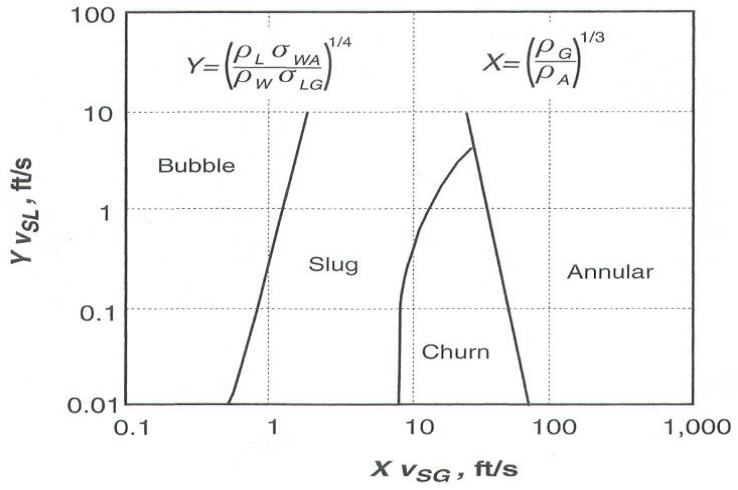

Figure 2.4 Generic flow map for vertical flow (Mandhane, 1984)

2.3 Introducing Junctions and Liquid-Liquid Phase Flow

The need to separate liquid-liquid flows is paramount and junctions are necessary configuration in a pipe network. Together and in the right combination a simple solution may be found to one of industries' largest capital costs in separating liquid-liquid flows. There are many variations of junction that exist but the simplest is where two pipes meet at right angles to one another and this is termed a 'T-junction'.

In the cases of two-phase flow the number of variables is much larger and is complicated by the constant mixing and splitting of the phases. The presence of dividing junctions creates further problems as either phase could pass preferentially into the branch.

2.4 The Simple T-junction

According to Wren (2001) the T-junction may be the simplest coupling together of two sections of pipe but there are many physical factors and dominant forces that affect how the two-phase flow approaching the junction may be divided between the outlets.

2.4.1 Dominant forces around T-junction

- ***Gravity***. The effect of gravitational acceleration acts predominantly on the liquid phase and can either promote liquid displacement down the branch arm, when it is oriented in a downwards direction help reduce liquid drawn off, when the branch arm is vertically upwards.
- ***Inertia***. The higher axial momentum flux of the liquid phase tends to force the liquid to continue flowing along the pipe, bypassing the entrance to the branch arm. This effect can be more pronounced when the diameter of the branch arm is smaller than the main run pipe. The liquid will pass the smaller opening quicker and thus have less time to be affected by any draw off effects.

- ***Pressure***. Pressure drop at the T-junction when the branch arm has a smaller diameter is larger compared to a T-junction where all branches are the same diameter.

2.4.2 Associated variables with T-junction

Wren (2001) also discussed about the geometrical properties of the T-junction can affect the flow split as well as the properties of the fluid flowing in the pipe. Such parameters include:

- The diameters of inlet, run and branch arms
- The inclination angles of the main pipe and side arm
- The angle of the junction and the radius of curvature where branch arm meets the main pipe

Besides that, according to Wren (2001), there are many variables beyond the physical geometry of the T-junction that must be considered when trying to predict what is likely to happen for a given flow pattern approaching the junction. The geometry includes the angles associated with the junction, the angle of the main pipe form the horizontal, the angle of the branch arm from the main pipe and the orientation of the branch arm, whether it lies in the horizontal plane, vertically upwards, vertically downwards or at angle In between.

2.5 Separation Efficiency

According to Yang *et al.* (2006), in order to optimize and access the phase separation results, a new criterion, separation efficiency has been proposed. Figure 2.5 shows the parameters need to be considered in defining the two-phase flow in T-junction. The $\dot{m}$ and $\dot{x}$ represent respectively the mass flow rate and kerosene mass quality; and subscripts K and W refer to kerosene and water, respectively. The inlet pipe is given the subscript 1, run arm 2, and the side arm 3.

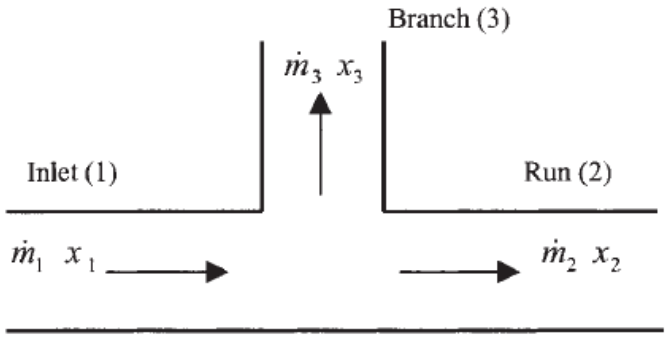

Figure 2.5 Parameters of two-phase flow at T-junction (Yang *et al*., 2006)

The results of phase separation at a T-junction are presented by using the fraction of one phase taken off versus another phase as shown in Figure 2.6. The fractions of kerosene and water taken off can be written as F_K and F_W, respectively as follows;

$$F_K = \frac{m_{K3}}{m_{K1}} \tag{1}$$

$$F_W = \frac{m_{W3}}{m_{W1}} \tag{2}$$

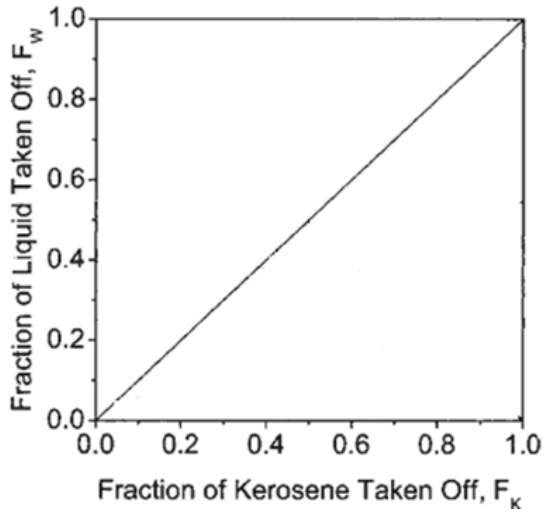

Figure 2.6 Separation efficiency derived from traditional expression for separation result. (Yang *et al*., 2006)

The abscissa is the fraction of kerosene taken off F_K, and the ordinate is the fraction of water taken off F_W. A diagonal line between (0,0) and (1,1) represents equal split, where there is no separation occurs if data lies on this line. This line divides the

figure area into two parts; data in the lower part correspond to kerosene flowing preferentially into the side-arm and vice versa. The further from the equal split line, the better the separation. The corner of this figure, (0,1) or (1,0) are conditions of complete separation. The distance L from the equal split line to a datum point, a good measure of the separation effected.

$$L = (F_K - F_W)\sin\alpha \tag{3}$$

$$\eta = \frac{L}{L_{\max}} = | F_K - F_W | \tag{4}$$

where α is the angle between the diagonal line and the abscissa. The separation efficiency Η] is now defined as the ratio of the actual separation to the complete separation.

2.6 Ideal Separation

Yang et al. (2006) stated that ideal phase separation occurs when two phase take off in the side-arm separately in order. Kerosene dominates the take off if data lie in the diagonally lower part of Figure 2.4, with water dominating when the data are in the diagonally upper part. For the point located exactly on the corner, pure kerosene and pure water are separated from the inlet mixture, respectively to the side arm and to the run arm. It means that the mass quality in the side arm $\dot{x}_3$ is equal to 1, and the quality in the run arm $\dot{x}_2$ is 0. Meanwhile, the separation efficiency reaches an ideal peak of 100%. When this ideal efficiency peak occurs, the fractional mass take off can be written as:

$$\frac{m_3}{m_1} = \chi_1 \tag{5}$$

For the first ideal separation line, pure kerosene emerges from the side arm and the mixture flows out from the run. It means that the fraction of water taken off F_W is 0, and the mass quality $\dot{x}_3$ is equal to 1. An equation can be derived for this line

$$\eta = F_K = \frac{1}{\chi_1}\frac{m_3}{m_1} \quad (\frac{m_3}{m_1} \le \chi_1) \tag{6}$$

Data lying on this line are associated with purer kerosene emerging through the side arm. Whereas for the second ideal line, pure water flows out from the run and the mixture emerges from the side arm. The quality in the run $\dot{x}_2$ is equal to 0. Similarly an equation for this ideal line can be derived as:

$$\eta = 1 - F_W = -\frac{1}{(1-\chi_1)}\frac{m_3}{m_1} + \frac{1}{1-\chi_1} \quad (\frac{m_3}{m_1} \geq \chi_1) \tag{7}$$

CHAPTER 3

METHODOLOGY

3.1 Development of Model Simulation

The development of a three dimensional T-junction model is built and the pipe length for inlet or main, run and side arms are all 50 millimeters and the corresponding diameters are all 50 millimeters too, as shown in Figure 3.1. The total volume of the T-junction is 400120 mm^3 and surface area is 36225 mm^2. Fine mesh is applied to the model and then followed by simulation using the CFD program solver (ANSYS Fluent). Parameters such as the velocity inlet for water and crude oil, inlet crude oil volume fraction, flow rate weighting for both outlets and others are taken into consideration.

This simulation applies the Eulerian multiphase model in ANSYS Fluent in modeling of two separate, yet interacting phases. In this study, we are using the continuity equations and the momentum balance equations. According to the mass conservative law, the continuity equation is:

$$\frac{\partial}{\partial t}(\alpha_k \rho_k) + \nabla \cdot (\alpha_k \rho_k u_k) = 0 \tag{8}$$

$$\sum_{k=1}^{N} \alpha_k = 1 \tag{9}$$

The conservative equation for the momentum can be expressed by:

$$\begin{aligned} &\frac{\partial}{\partial t}(\alpha_k \rho_k u_k) + \nabla \cdot (\alpha_k \rho_k u_k u_k) = \\ &-\nabla(\alpha_k p) - \nabla \cdot \tau_k + \alpha_k \rho_k g + \alpha_k \rho_k \cdot (F_k + F_{lift,k} + F_{vm,k}) + K_{kl}(u_k - u_l) \end{aligned} \tag{10}$$

In case the particle diameter is relatively large, the following lift force must be taken into account:

$$F_{lift} = -0.5\alpha_k \rho_k |u_k - u_l| \times (\nabla \times u_l) \tag{11}$$

Due to the acceleration of the secondary phase to the primary phase, a virtual mass force on the particles should also be considered, defined by:

$$F_{vm} = 0.5\alpha_k \rho_k \left(\frac{du_l}{dt} - \frac{du_k}{dt}\right)_l \tag{12}$$

The exchange coefficient K_{kl} for oil/water two-phase flow can be written in the following general form:

$$K_{kl} = \frac{\alpha_k (\alpha_k \rho_k + \alpha_l \rho_l) f}{\tau_{kl}} \tag{13}$$

herein, τ_{kl} is the particulate relaxation time and f the drag function, defined as:

$$\tau_{kl} = \frac{(\alpha_k \rho_k + \alpha_l \rho_l)\left(\frac{d_k + d_l}{2}\right)^2}{18(\alpha_k u_k + \alpha_l u_l)} \tag{14}$$

$$f = \frac{C_D \,\mathrm{Re}}{24} \tag{15}$$

$$C_D = \frac{24(1 + 0.15\,\mathrm{Re}^{0.687})}{\mathrm{Re}}, \mathrm{Re} \le 1000 \tag{16}$$

$$C_D = 0.44, \mathrm{Re} > 1000 \tag{17}$$

$$\mathrm{Re} = \frac{\rho_k |u_k - u_l| d_k}{\mu_k} \tag{18}$$

Currently several types of turbulence models can be applied to describe the effects of turbulent fluctuations of velocities and scalar quantities in multiphase flow, of which the

mixture $k-\varepsilon$ model is applicable in case the phase density ratio close to unit. In this model k and ε equations are as follows:

$$\frac{\partial}{\partial t}(\rho_m k)+\nabla\cdot(\rho_m u_m k)=\nabla\cdot(\frac{\mu_{t,m}}{\sigma_k}\nabla k)+G_{k,m}-\rho_m\varepsilon \tag{19}$$

$$\frac{\partial}{\partial t}(\rho_m \varepsilon)+\nabla\cdot(\rho_m u_m \varepsilon)=\nabla\cdot(\frac{\mu_{t,m}}{\sigma_\varepsilon})+\frac{\varepsilon}{k}(C_{1\varepsilon}G_{k,m}-C_{2\varepsilon}\rho_m\varepsilon) \tag{20}$$

where the mixture density ρ_m and the mixture velocity u_m are defined as:

$$\rho_m=\sum_{k=1}^{N}\alpha_k\rho_k \tag{21}$$

$$u_m=\frac{\sum_{k=1}^{N}\alpha_k\rho_k}{\sum_{k=1}^{N}\alpha_k\rho_k} \tag{22}$$

The turbulent viscosity μ_t and the production of turbulence kinetic energy $G_{k,m}$ can be computed from:

$$\mu_{t,m}=\rho_m C_\mu\frac{k^2}{\varepsilon} \tag{23}$$

$$G_{k,m}=\mu_{t,m}[\nabla u_m+(\nabla u_m)^T]:\nabla u_m \tag{24}$$

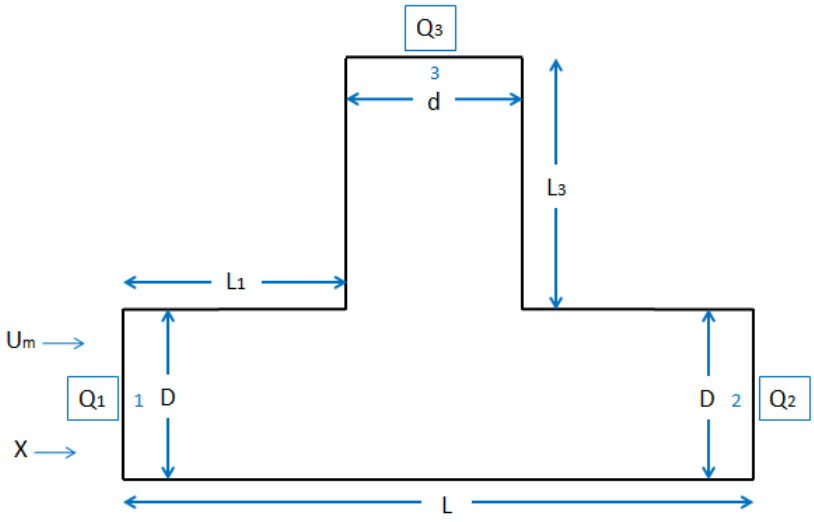

Figure 3.1 Schematic T-junction with applied inlet and outlets boundary conditions

Table 3.1 illustrates the input parameters for validations from Yang *et al.* (2007) experiment data. The lowest and highest limit range for parametric studies have been set and listed in Table 3.1 in order to have clearer view on how the parameters above affect the phase separation.

Table 3.1 Input parameters for validations and parametric studies

Input Parameters	Validations	Present Study
Main and run arm diameter, D (mm)	50	50
Side arm diameter, d (mm)	50	25-50
Length of main and run arm, L_1 (mm)	500	500
Length of side arm, L_3 (mm)	500	250-500
Density of water phase, ρ_w (kg/m^3)	998.2	998.2
Density of oil phase, ρ_o (kg/m^3)	828 (kerosene)	626 - 828
Inlet mixture velocity, U_m (m/s)	0.27, 0.28, 0.56, 1.19	0.2-0.8
Overall mass split ratio, Q	0.2, 0.4, 0.6, 0.8	0.2, 0.4, 0.6, 0.8
Operating pressure, P (kPa)	101.325	101.325
Inlet volume fraction of oil phase, α_o	0.23	0.2-0.8
Averaged bubble diameter (m)	0.0004	0.0004

3.2 Mesh Dependency Analysis Check

This analysis is one of the approaches used to study the convergence behavior based on the mesh density. In order to do so, several runs of simulation had been performed with varying total number of tetrahedral cells. The pressure distribution in the T-junction is the criteria selected to check on the convergence behavior in this study. Figure 3.2 and Figure 3.3 illustrate the convergence behavior of different mesh density based on the pressure obtained at a particular point or position at the T-junction model. For the coarser meshes or lower mesh density, the pressure distribution at a particular point increases initially. In other words, the error on the coarser mesh is high and it is mainly influenced by the mesh density. The curve converges as the mesh is refined and it provides much better resolution compared to a coarser mesh. The present approach resulted in approximately two hours per simulation time.

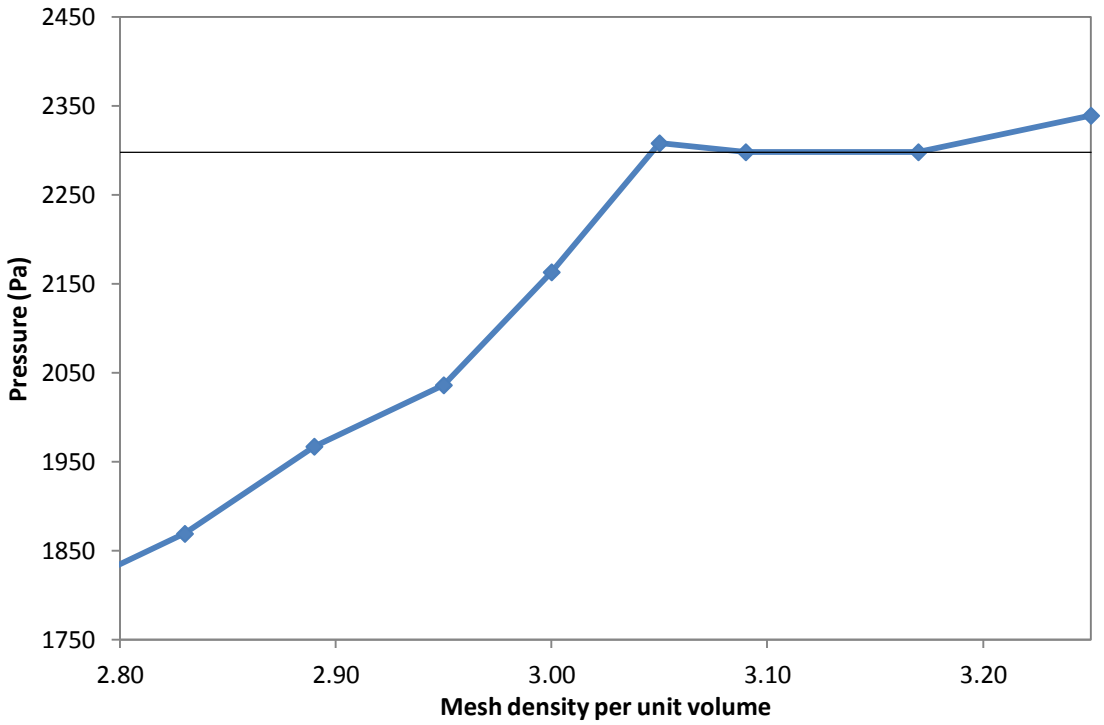

Figure 3.2 Graph of pressure convergence versus mesh density

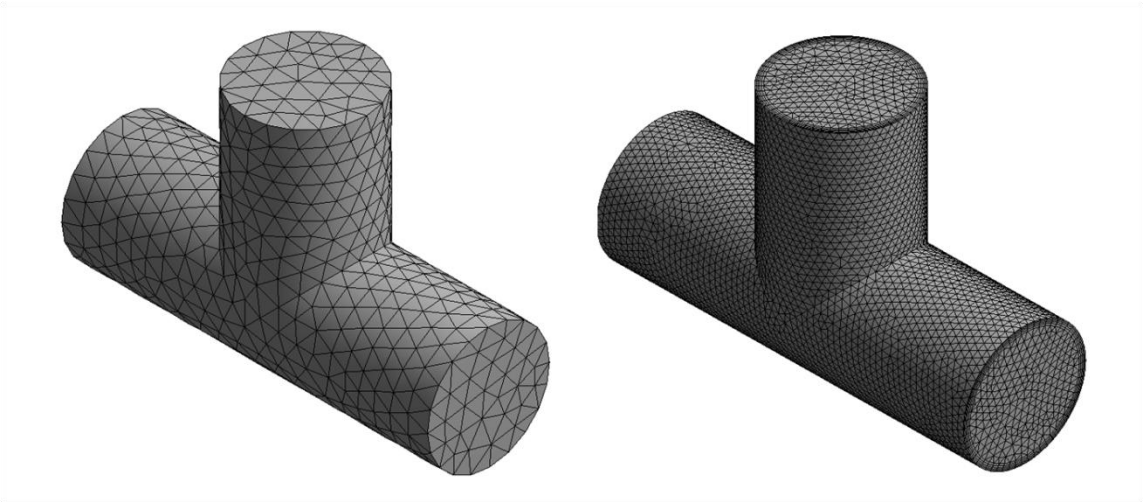

Figure 3.3 Computational mesh refinement of T-junction

All the figures below illustrate the contours of the fluid phases in T-junction. Basically, the comparison are made between the coarsest mesh and the finest mesh which have total number of 25128 tetrahedral cells and total number of 160099 tetrahedral cells respectively. It is shown that the contours differ from the coarsest and the finest meshes. These depict that the contours are more precise and accurate as the mesh is refined.

3.2.1 Comparison of mixture phase pressure contour by applying different mesh densities

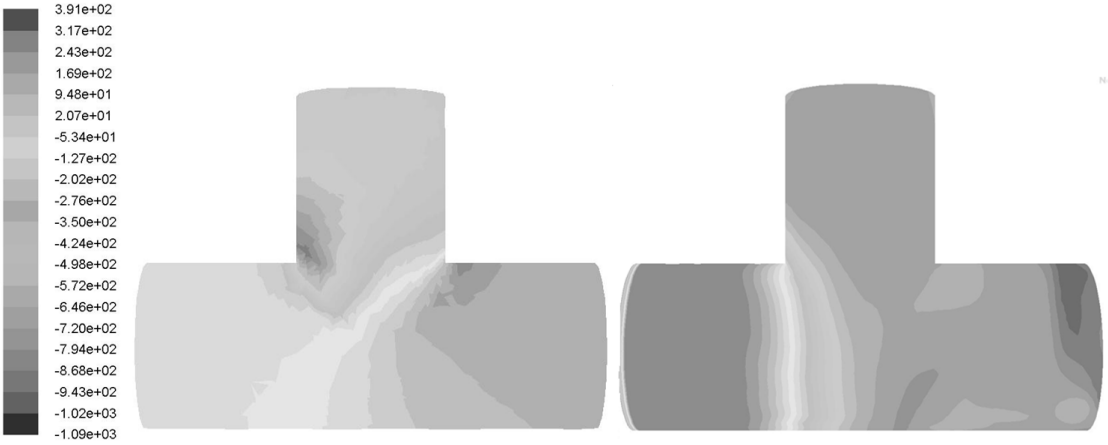

Figure 3.4 Pressure contour of mixture phase with total number of 25128 tetrahedral cells and 160099 tetrahedral cells

3.2.2 Comparison of water phase velocity streamline by applying different mesh densities

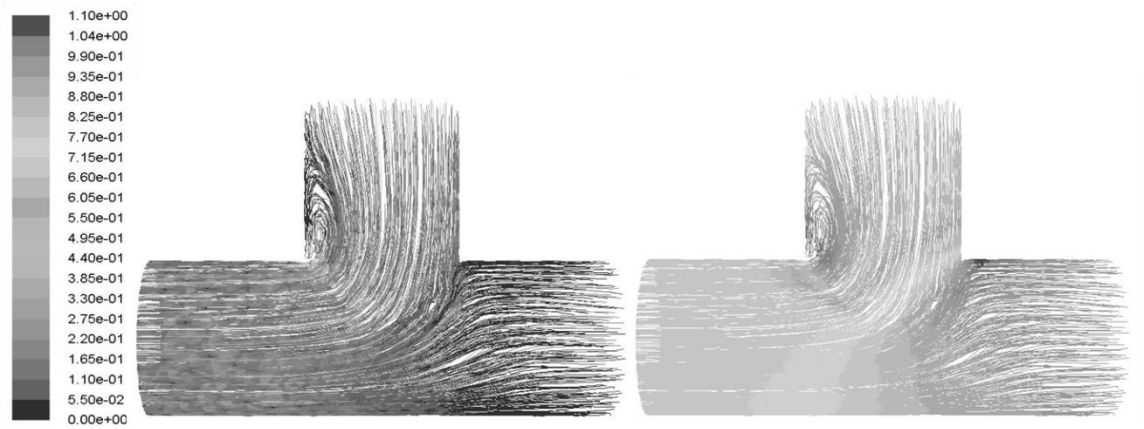

Figure 3.5 Velocity streamline of water phase with total number of 25128 tetrahedral cells and 160099 tetrahedral cells

3.2.3 Comparison of oil phase velocity contour by applying different mesh densities

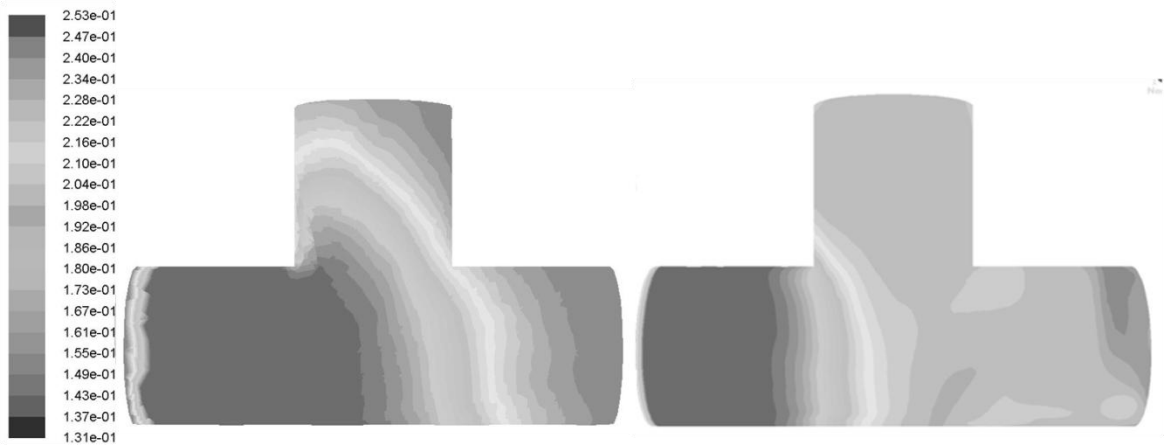

Figure 3.6 Velocity of oil phase with total number of 25128 tetrahedral cells and 160099 tetrahedral cells

3.3 Project Methodology and Activities

Figure 3.7 shows the project phases of the whole study. The project is divided into four phases which are the background study and literature review, T-junction modeling, model simulation and lastly the simulation results analysis and validations.

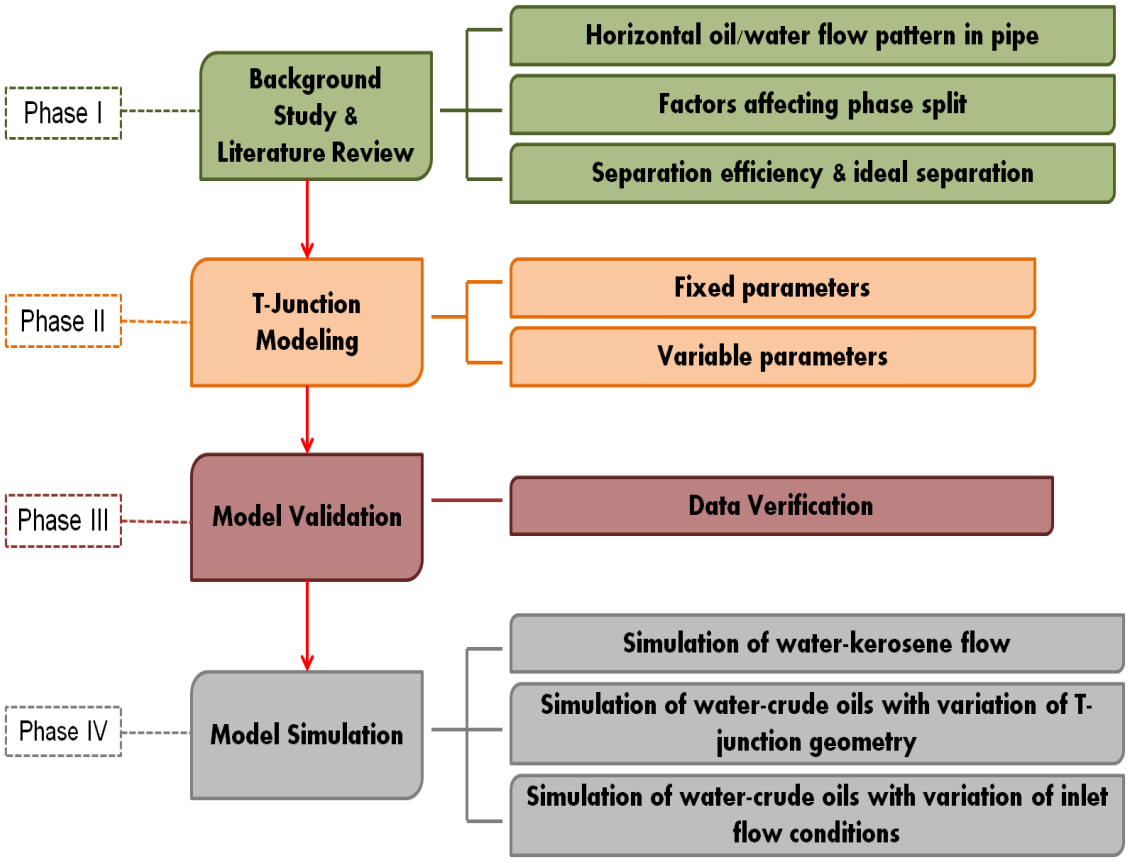

Figure 3.7 Four phases of project methodology & activities

3.4 Gantt Chart and Key Milestones for FYP I

Table 3.2 Gantt chart and milestones for FYP I and FYP II

Detail/Week	1	2	3	4	5	6		8	9	10	11	12	13	14
Selection of Project Topic														
Literature Review						▲								
Prelim Report submission							MID-TERM BREAK							
Familiarization with FLUENT software.														
Gather information to model the T-Junction									▲					
Methodology Studies														
Proposal Defense and progress evaluation														
T-Junction modeling construction with FLUENT										▲				
Gather and analyze results obtained														
Draft interim report submission														
Full scale interim report														

Legend :- Process ▲ Key Milestones

3.5 Gantt Chart and Key Milestones for FYP II

Table 3.3 Gantt chart and milestones for FYP II

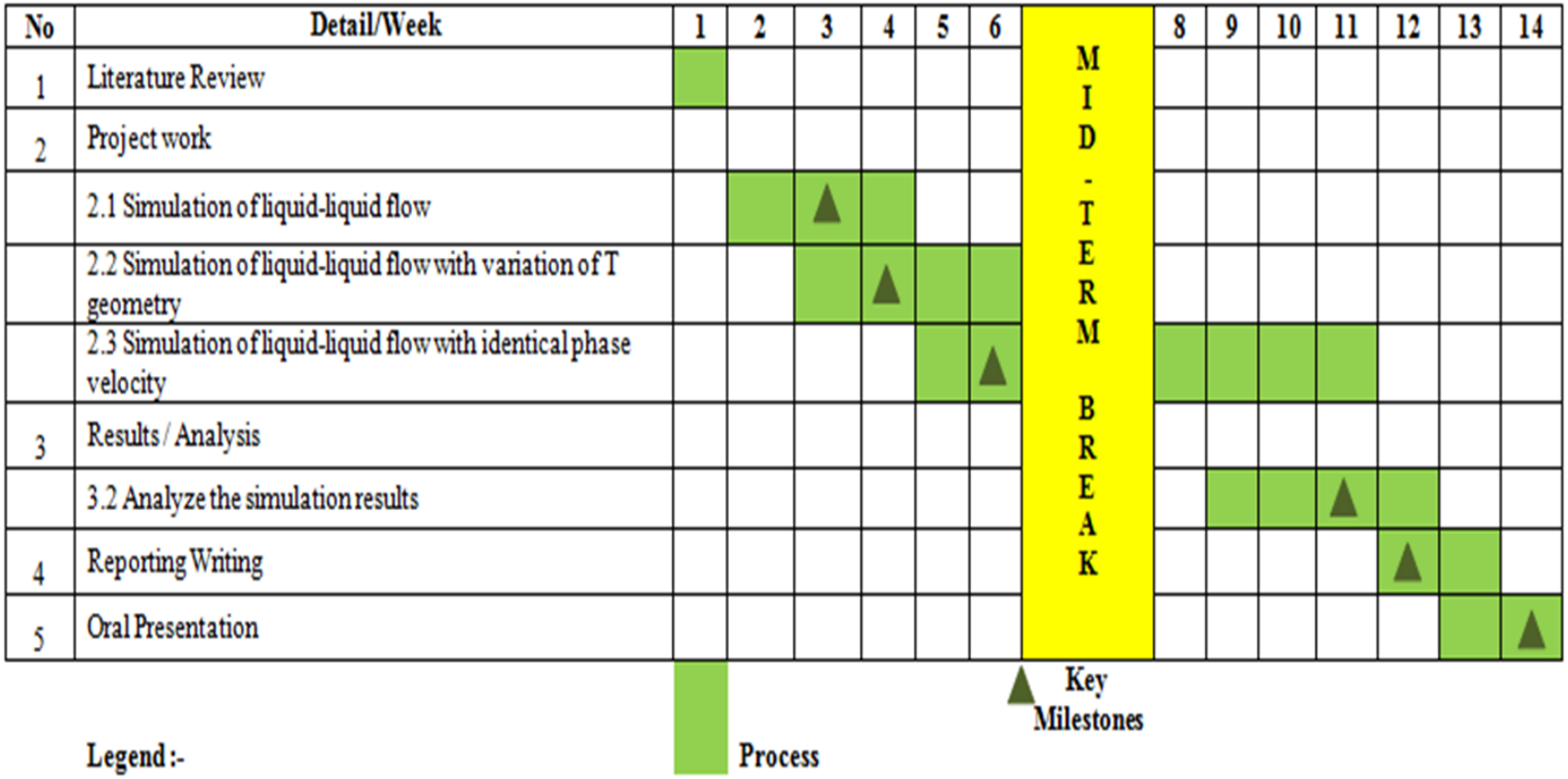

3.6 Tools Required

FLUENT is software for modeling fluid flow and heat transfer in complex geometries. It is ideally suited for both incompressible and compressible fluid-flow simulations. This software is also able to provide complete mesh flexibility including the ability to solve flow problems. This project requires FLUENT software to build the T-junction model and simulate two-phase flow splitting in T-junction.

CHAPTER 4

RESULTS AND DISCUSSIONS

4.1 Verification of the Simulation Model with Experiment Data

Yang *et al.* (2005) did an experiment to study the flow split behavior in a T-junction which provide the experiment data comparing the flow split efficiency in terms of the oil taken off value and the water taken off value. In this experiment set-up, a mixture of water and kerosene was introduced into a T-junction with a 50mm pipe diameter for all arms. The main arm was arranged vertically and the side arm was made horizontal.

A uniform velocity profile is imposed for both water and kerosene phases at the inlet boundary, which all data samples are selected from Yang's experiments. α_k refers to the volume of kerosene fraction while U_m refers to the averaged inlet mixture velocity which is calculated according to:

$$U_{\mathrm{m}} = \frac{\alpha_{\mathrm{w}}\rho_{\mathrm{w}}u_{\mathrm{w}} + \alpha_{\mathrm{k}}\rho_{\mathrm{k}}u_{\mathrm{k}}}{\alpha_w\rho_w + \alpha_k\rho_k} \tag{24}$$

where ρ_w and ρ_k refer to the density of water and kerosene respectively. The detailed values of input parameters are provided in Methodology chapter, Table 3.1.

In this study, the measured overall flow split, Q_3/Q_1 is specified and this leaves the individual phase flow split to be predicted as an outcome. Lastly, no slip type is applied to the boundary condition for the tube wall. The flow parameters of four inlet flow conditions were investigated and analyzed where each flow conditions consists of four groups of overall mass split ratio which are 0.2, 0.4, 0.6 and 0.8.

The data collected from the Pandey *et al*.'s experiment is used to compare with the data collected from the simulation model on the similar case. Figure 4.1 shows the T-junction built with 500mm for all arms with 50mm of diameter.

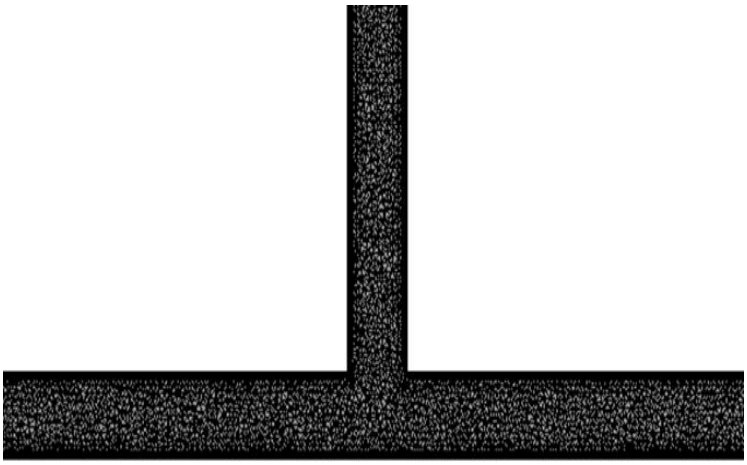

Figure 4.1 Computational grid of T-junction

In order to verify the above model, the oil-water two phase flow inside a horizontal T-junction is numerically simulated and four different predicted flow conditions are used. In run#1, the mixture velocity is v=0.27m/s and the oil volumetric fraction α=21%, in run#2 v=0.28m/s and α=23%, in run#3 v=0.56m/s and α=22%, while in run#4 v=1.19m/s and α=21%. The results are compared with the experimental data obtained by Pandey *et al*. Figure 4.2 shows that the simulation results agree well with the experimental data. The Eulerian multi-fluid model and the mixture *k* model can satisfy the need of the simulation of the T-junctions completely.

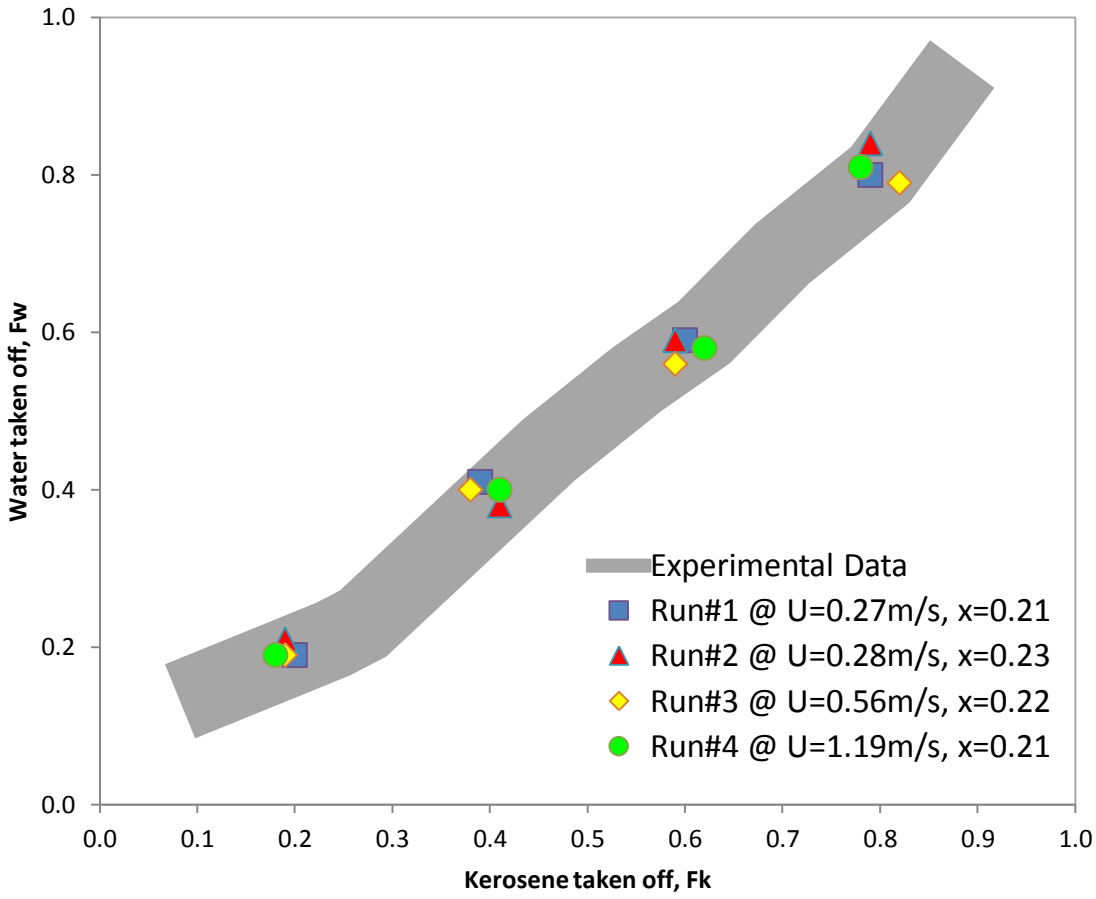

Figure 4.2 Simulated flow split curves compared with experimental results

4.2 Parametric Studies on Two-Phase Separation Efficiency in T-junction

By using simulation model that has been developed, five factors are examined which are predicted to be affecting the two-phase separation efficiency through several parametric studies for T-junction. Those variables are the diameter ratio and the length ratio of side arm to the main arm, density ratio, initial mixture velocity ratio of the fluids and inlet oil fraction. Detailed parameters of simulation model are summarized in Table 3.1 under Methodology chapter. With the listed parameters range, the resulting fraction of oil taken off is clearly shown as figures below according to the variation of input parameters.

4.2.1 Effect of Diameter Ratio on Fraction of Oil Taken Off

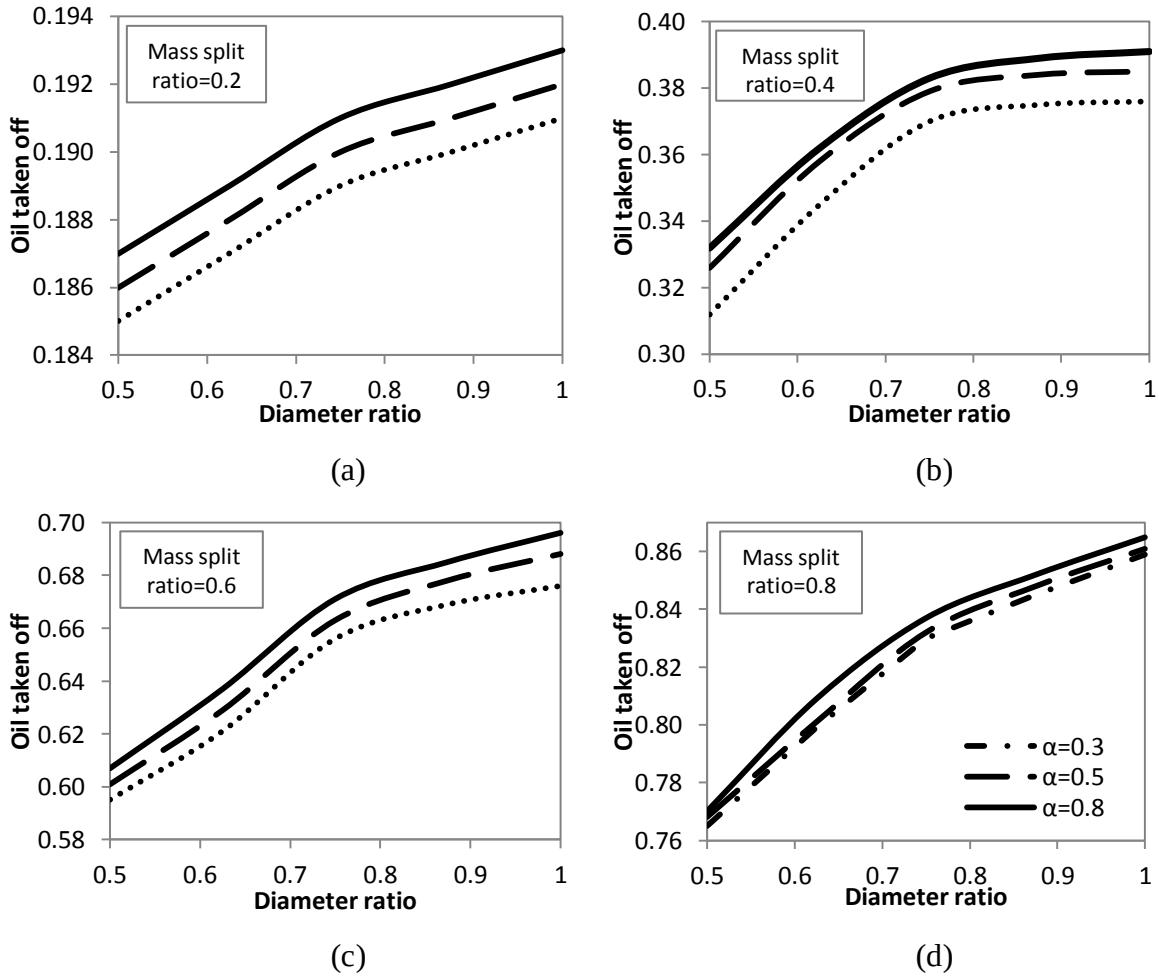

Figure 4.3 Effect of diameter ratio on fraction of oil taken off with initial velocity of 0.4m/s and pentane density of 626kg/m^3

Based on Figure 4.3, the gradient of each section of the line refers to the fraction of oil taken off per unit change of diameter ratio for mass split ratio, M of 0.20, 0.40, 0.60 and 0.80 with inlet oil ratio, α of 0.30, 0.50 and 0.80, are summarized as Table 4.1.

Table 4.1 Fraction of oil taken off per unit change of diameter ratio for mass split ratio, M of 0.20, 0.40, 0.60 and 0.80.

Inlet Oil Ratio, α	**Diameter Ratio, D**	**Gradient**			
		M = 0.2	**M = 0.4**	**M = 0.6**	**M = 0.8**
0.30	0.50 to 0.75	0.016	0.232	0.244	0.260
	0.75 to 1.00	0.008	0.024	0.08	0.116
0.50	0.50 to 0.75	0.016	0.212	0.248	0.256
	0.75 to 1.00	0.008	0.024	0.100	0.116
0.80	0.50 to 0.75	0.016	0.204	0.256	0.268
	0.75 to 1.00	0.008	0.0.32	0.100	0.112

Based on Table 4.1, it shows that the fraction of oil taken off increases as the diameter ratio increases from 0.50 to 0.75 and results in an increase of fraction of oil taken off per unit change of diameter. However, the effect of diameter ratio on fraction of oil taken off is diminishing as the diameter ratio increases from 0.75 to 1.00 which results in a small gradient. As for mass split ratio of 0.80, it is shown that it has highest gradient among the mass split ratio of 0.20, 0.40, 0.60 and 0.80 which result in greatest fraction of oil taken off per unit change of diameter ratio. In other words, the change of gradient of M = 0.20 and 0.40 implies the fraction of oil taken off per unit of diameter ratio per mass split ratio radically especially when the initial oil ratio of 0.30. The fraction of gas taken off increases from diameter ratio of 0.50 to 0.75 too for mass split ratio of 0.80 which results in an increase of fraction of oil taken off per unit change of diameter ratio. In brief, Figure 4.3 depicts the optimum performance of a T-junction takes place when the diameter ratio of side arm to main arm is reduced to about 0.75 where maximum fraction of oil is taken off. This is where it reaches the inflection point where the fraction of oil taken off will slowly increase.

4.2.2 Effect of Inlet Oil Ratio on Fraction of Oil Taken Off

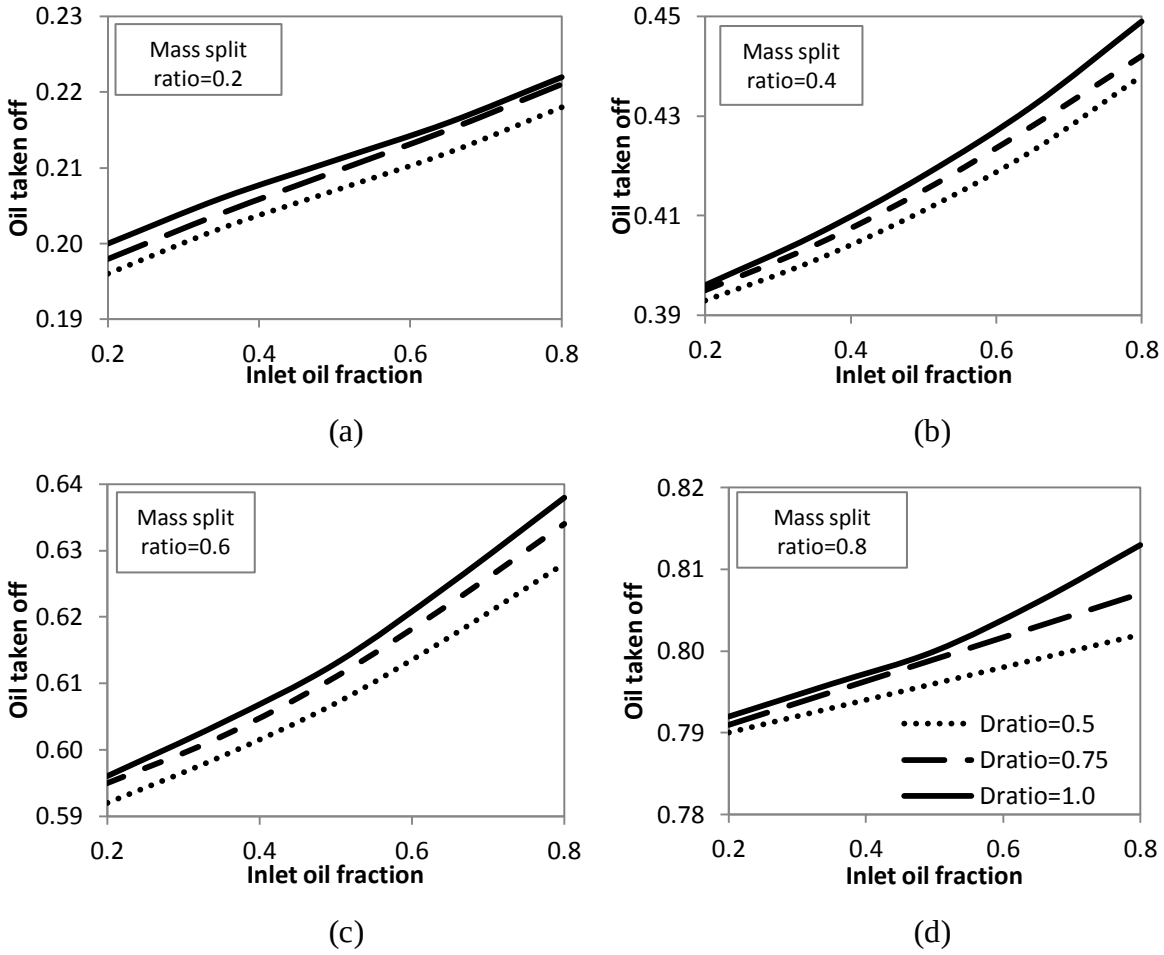

Figure 4.4 Effect of inlet oil fraction on fraction of oil taken off with initial mixture velocity of 0.4m/s and oil density of 626kg/m^3

Based on figure above, the gradient of each section of the line which refers to the fraction of oil taken off per unit change of inlet oil fraction with variation of diameter ratio is summarized as Table 4.2.

Table 4.2 Fraction of oil taken off per unit change of inlet oil fraction for mass split ratio, M of 0.20, 0.40, 0.60 and 0.80

Diameter Ratio, D	Inlet Oil Ratio, α	Gradient			
		M = 0.2	M = 0.4	M = 0.6	M = 0.8
0.50	0.20 to 0.50	0.037	0.060	0.050	0.020
	0.50 to 0.80	0.037	0.090	0.070	0.020
0.75	0.20 to 0.50	0.038	0.067	0.053	0.027
	0.50 to 0.80	0.038	0.027	0.078	0.027
1.00	0.20 to 0.50	0.037	0.073	0.057	0.027
	0.50 to 0.80	0.037	0.103	0.083	0.043

Based on the Table 4.2, it shows that the fraction of oil taken off increases as the inlet oil fraction increases from 0.20 to 0.80 and results in a slight increase of fraction of oil taken off per unit change of inlet oil ratio. From Figure 4.4 (a), (b), (c) and (d), it is clearly illustrated the fraction of oil taken off is significantly less for diameter ration of 0.50 compared to diameter ratio 0.75 and 1.00. Basically, Figure 4.4 (a), (b) and (c) show the effect of inlet oil fraction on fraction of oil taken off are same as the gradient for mass split ratio, M of 0.20, 0.40 and 0.60 does not have very much difference. However, for Figure 4.4 (c), there is a minor which indicates the inlet oil ratio does affect on the fraction of oil taken off when mass split ratio, M of 0.80 and it is proven in Table 4.2 where the gradient for inlet oil ratio from 0.50 to 0.80 for diameter ratio of 1.00 have a abrupt increase compared to mass split ratio, M of 0.20, 0.40 and 0.60. In another word, inlet oil ratio does affect the fraction of oil taken off only when the overall mass split ratio is 0.80 whereby the diameter ratio is 1.00.

4.2.3 Effect of Pipe Length Ratio on Fraction of Oil Taken Off

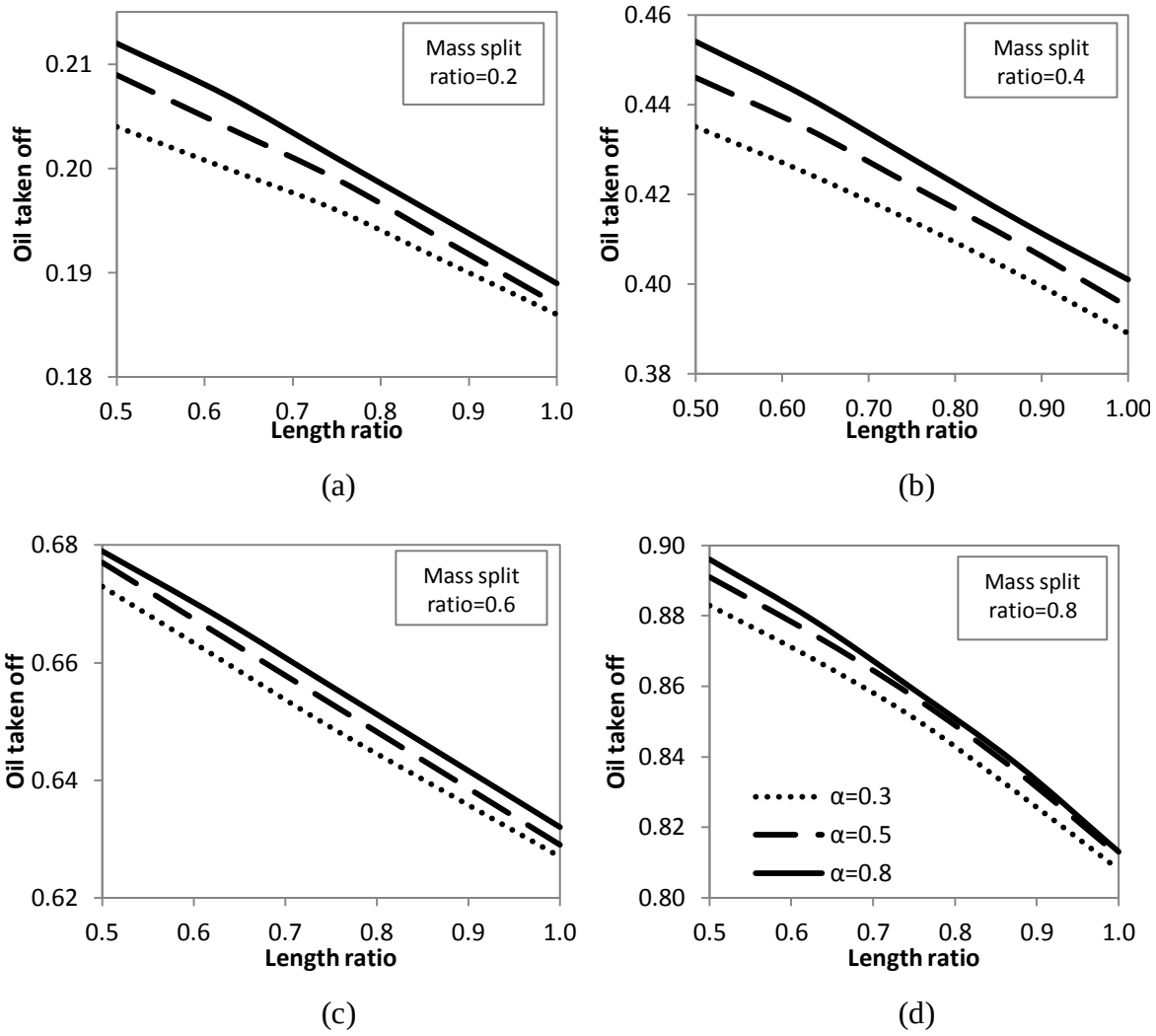

Figure 4.5 Effect of length ratio on fraction of oil taken off with initial mixture velocity of 0.4m/s and oil density of 626kg/m^3

Based on Figure 4.5, the gradient of each section of the line which refers to the fraction of oil taken off per unit change of length ratio with variation of inlet oil ratio is summarized as Table 4.3.

Table 4.3 Fraction of oil taken off per unit change of length ratio for mass split ratio, M of 0.20, 0.40, 060 and 0.80.

Inlet Oil Ratio, α	Length Ratio, L	Gradient			
		M = 0.2	**M = 0.4**	**M = 0.6**	**M = 0.8**
0.30	0.50 to 0.75	-0.032	-0.084	-0.096	-0.128
	0.75 to 1.00	-0.040	-0.100	-0.088	-0.172
0.50	0.50 to 0.75	-0.040	-0.096	-0.096	-0.136
	0.75 to 1.00	-0.048	-0.108	-0.096	-0.180
0.80	0.50 to 0.75	-0.044	-0.104	-0.092	-0.148
	0.75 to 1.00	-0.048	-0.108	-0.096	-0.184

Based on the Table 4.3, it shows that the fraction of oil taken off decreases as the length ratio increases from 0.50 to 1.00 and results in a great decrease of fraction of oil taken off per unit change of length ratio. From Figure 4.5 (d), it is clearly illustrated that the fraction of oil taken off is significantly less for mass split ratio, M of 0.80 compared to M of 0.20, 0.40 and 0.60 which do not have much difference. From Table 4.3 it is proven that gradient for length ratio from 0.75 to 1.00 do have a great differences for mass split ratio, M of 0.80 compared to M = 0.20, 0.40 and 0.60. This proves that the effect of pipe length ratio affect the phase separation efficiency.

4.2.4 Effect of Mixture Velocity Ratio on Fraction of Oil Taken Off

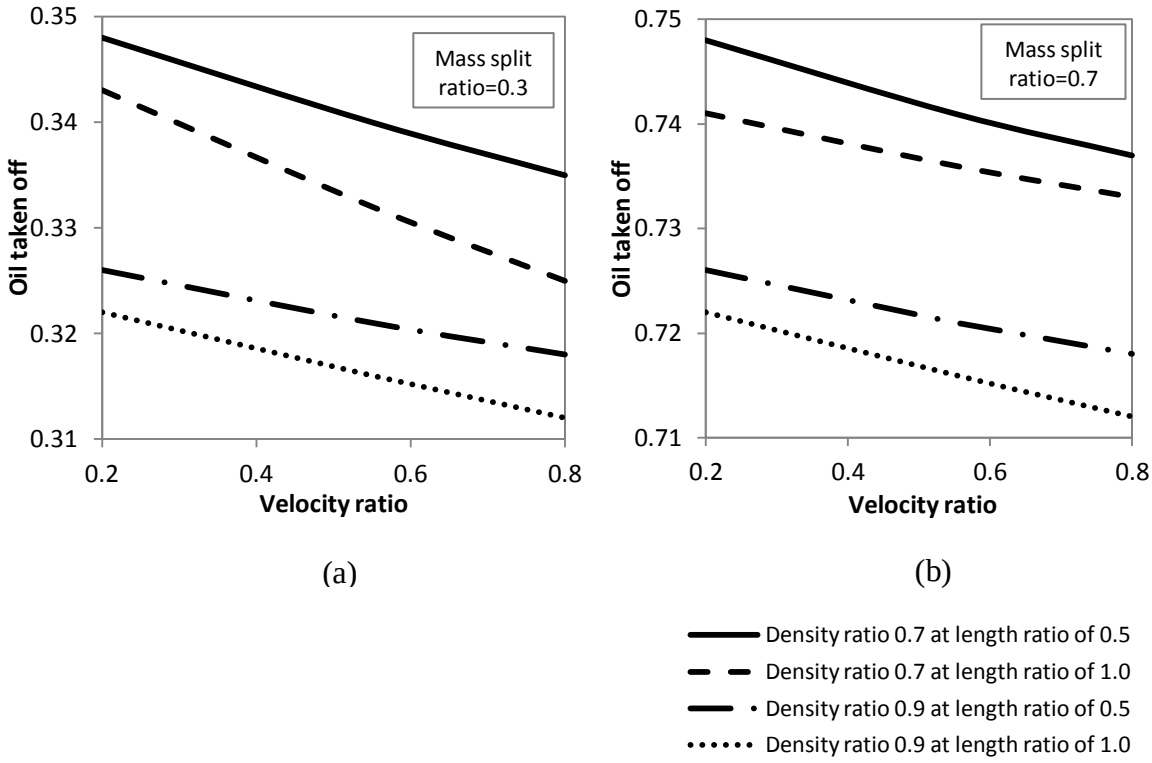

Figure 4.6 Effect of mixture velocity ratio on fraction of oil taken off at density ratio of 0.70 and 0.90, and length ratio of 0.50 and 1.00

The effect of per unit change of velocity ratio on the fraction of oil taken off with variation of density ratio and length ratio of 0.50 and 1.00 for mass split ratio, M of 0.30 and 0.70 is summarized as Table 4.4.

Table 4.4 Fraction of oil taken off per unit change of velocity ratio with variation of density ratio and length ratio for mass split ratio of 0.30 and 0.70

Density Ratio, ρ	**Length Ratio, L**	**Velocity Ratio, U**	**Gradient**	
			M = 0.3	**M = 0.7**
0.70	0.50	0.20 to 0.80	-0.022	-0.018
	1.00	0.20 to 0.80	-0.030	-0.013
0.90	5.00	0.20 to 0.80	-0.013	-0.013
	1.00	0.20 to 0.80	-0.014	-0.017

Figure 4.6 (a) and (b) illustrates the effect of fluid velocity ratio is inversely proportional to the fraction of oil taken off. From Table 4.4, it summarizes that the gradient decreases from velocity ratio 0.20 to 0.80 when length ratio increases from 0.50 to 1.00 for both mass split ratio, M of 0.30 and 0.70 at density 0.70. In the other hand, velocity ratio has a greater effect when the length ratio increases from 0.50 to 1.00 when the density is at 0.90 for both mass split ratio, M of 0.30 and 0.70. This shows that the density ratio does affect the phase separation efficiency of oil taken off per unit change of fluid velocity ratio.

4.2.5 Effect of Density Ratio on Fraction of Oil Taken Off

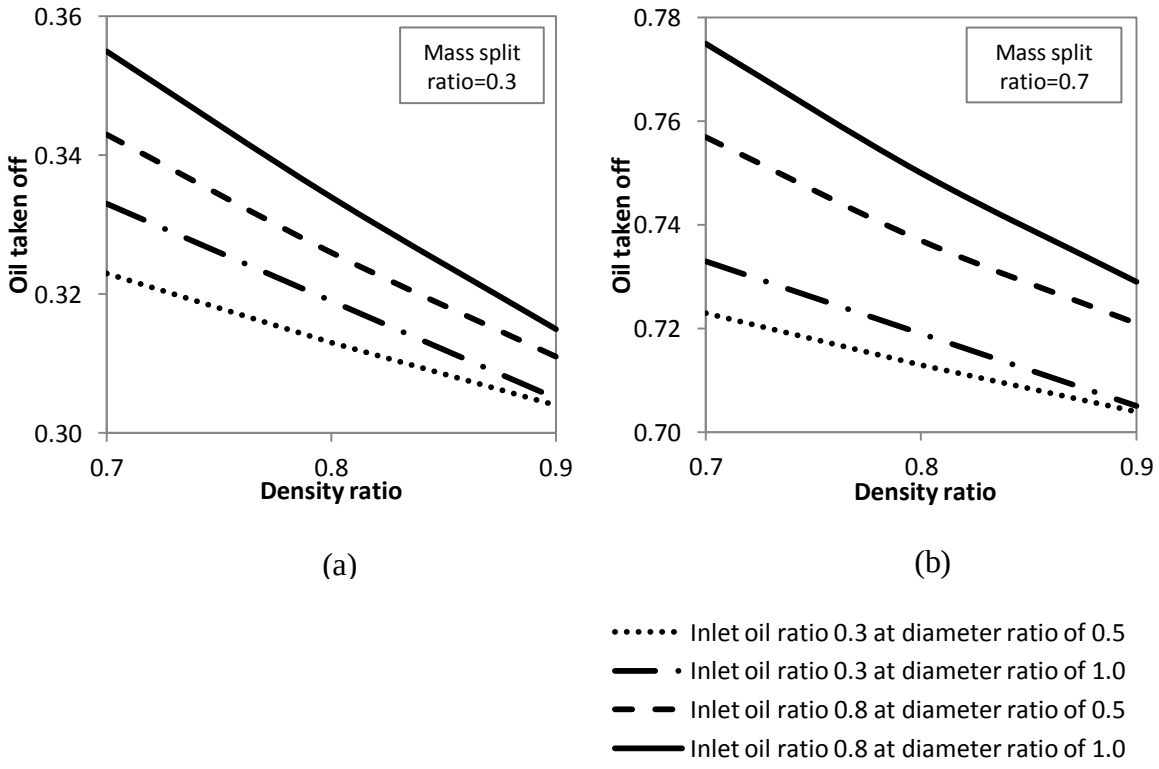

(a) (b)

Figure 4.7 Effect of density ratio on fraction of oil taken off at inlet oil ratio of 0.30 and 0.80, and diameter ratio of 0.50 and 1.00

The effect of per unit change of density ratio on the fraction of oil taken off with variation of inlet oil ratio and diameter ratio for mass split ratio, M of 0.30 and 0.70 is summarized as Table 4.5.

Table 4.5 Fraction of oil taken off per unit change of density ratio with variation of inlet oil ratio and diameter ratio for mass split ratio of 0.30 and 0.70

Inlet Oil Ratio, α	Diameter Ratio, D	Density Ratio, ρ	Gradient	
			M = 0.3	M = 0.7
0.30	0.50	0.70 to 0.90	-0.095	-0.095
	1.00	0.70 to 0.90	-0.140	-0.140
0.80	5.00	0.70 to 0.90	-0.160	-0.180
	1.00	0.70 to 0.90	-0.200	-0.230

Figure 4.7 (a) and (b) illustrates the effect of density ratio is inversely proportional to the fraction of oil taken off. From Table 4.5, it summarizes that the density ratio has a greater effect when the diameter ratio increases from 0.50 to 1.00 when the inlet oil ratio increases from 0.30 to 0.80. This proves that the effect of density ratio does affect the phase separation efficiency when the inlet oil ratio is high. On top of that, the table also implies the fraction of oil taken off per unit change of density ratio per mass split ratio increases for both diameter ratio and inlet oil ratio.

4.3 Concluding Remarks

Based on the parametric findings, density ratio plays the most important role on phase separation. This parameter refers to the density ratio of oil phase to water phase, by varying the density of oil phase while water phase density is remain constant. It is also clearly proven that the density ratio dominates the fraction of gas taken off. On the other hand, inlet oil fraction does play as the least important role on phase separation in T-junction. However, further investigation of this effect with variation of operating condition is required to have clearer picture on effect of inlet oil ratio on flow splitting behavior in T-junction.

Since the phenomenon of phase misdistributions is utilized to separate the phases in different proportions among the outlet arms, hence as discussed in the literature review the working fluids' density differences does affect the separation performance in T-junction. Theoretically, the lesser dense fluid will tend to divert to the side arm while the denser fluid will tend to remain at the main and run arms. From the findings, it is proven that the larger the density differences of working fluids, more oil will tend to divert to the side arm and results in greater fraction of oil taken off. Hence, this depicts that the theoretical study on phase splitting phenomenon is verified.

When dealing with a large number of parameters in solving an engineering problem, it is better to determine the more significant parameters of the outcome. Based on the parametric studies above, Figure 4.10 summarizes the weighting factors in percentage to the applied equations from lowest to highest upon the fraction of oil taken off. It illustrates that density ratio does the most impact on the phase separation, and then followed by the mixture velocity ratio and length ratio. Conversely, both diameter ratio and inlet oil ratio have the least impact compared to the rest of the parameters. This figure also implies the proportionality in terms of mathematical relation and it shows that the diameter ratio and the inlet oil fraction are the directly proportional to the fraction of oil taken off while the length ratio, inlet mixture velocity and the fluid density differences is inversely proportional to the fraction of oil taken off in T-junction.

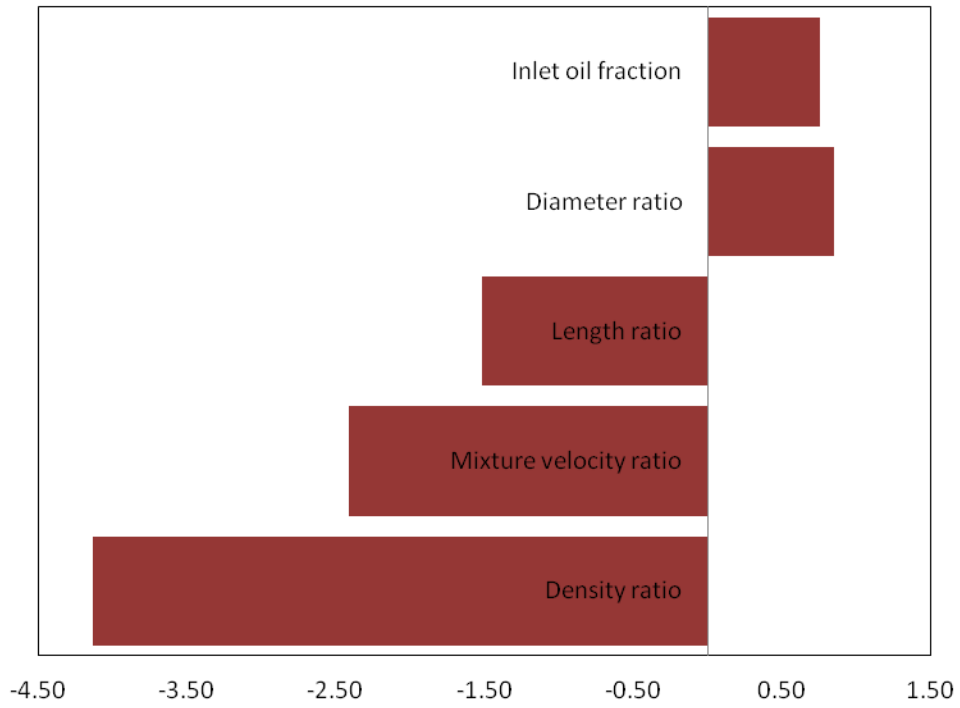

Figure 4.8 Parameters' weighting factor on two-phase separation in T-junction

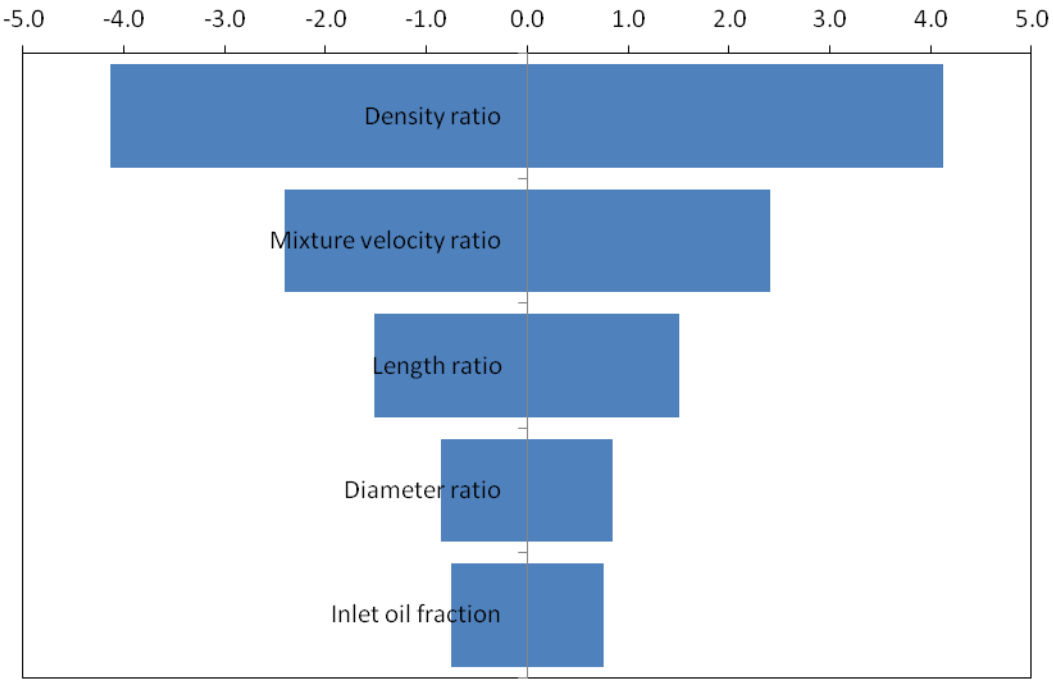

Figure 4.9 Parameters' sensitivity to fraction of oil taken off

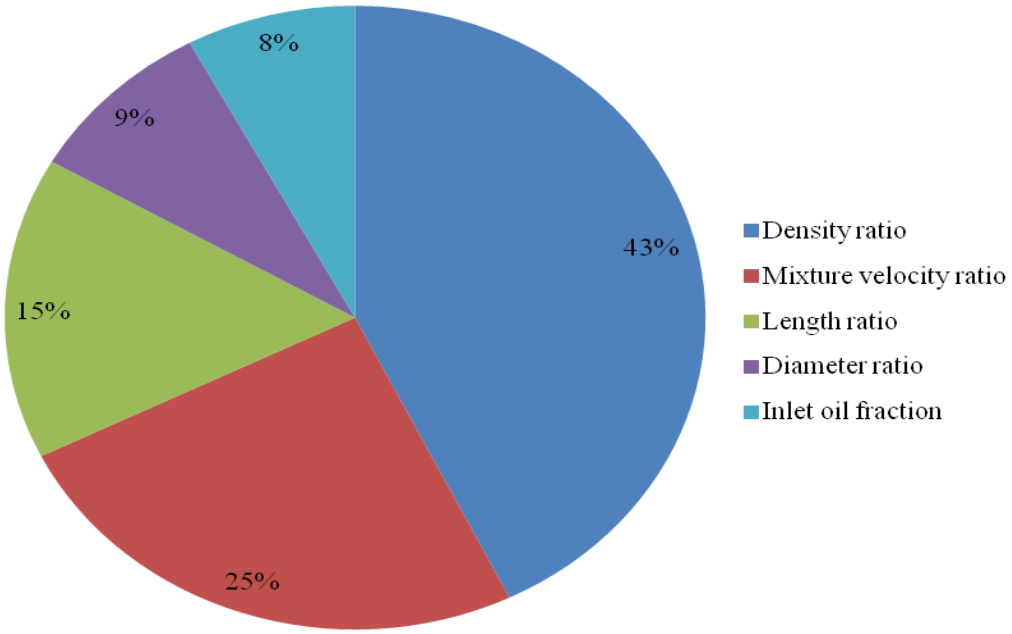

Figure 4.10 Parameters' weighting factor based on percentage

In order to look at the parameters' sensitivity, tornado chart is constructed as shown in Figure 4.9. This chart clearly illustrates the sensitivity of parameters to the solution. It reveals that the most sensitive parameters are the density ratio, mixture velocity ratio and length ratio where all of these factors have the affecting percentage of 83% out of the five parameters as illustrate in Figure 4.10. The least sensitive parameters include the diameter ratio and inlet oil fraction which contribute 9% and 8% respectively towards the parameters affecting the phase separation in T-junction.

CHAPTER 5

CONCLUSIONS AND RECOMMENDATIONS

T-junctions are very common within pipe networks, mainly involving in splitting or mixing the fluids especially in the petroleum industry. In order to obtain a better separation performance for optimal operation of downstream components from the junction, it is very essential effort to understand the efficiency of the phase separation and the geometric effect of the T-junction on the flow split. This study is mainly focus on phase separation in t-junction with horizontal main arm and vertical side arm using crude oil and water as working fluids.

Using the developed simulation model, the significance of associated parameters on two-phase separation efficiency in T-junction is studied. The diameter ratio, inlet oil fraction, length ratio, mixture velocity ratio and density ratio are identified as the main factors affecting the fraction of oil taken off in T-junction. It is found that among these parameters, the most influential factor is the density ratio of oil phase to water phase. As discussed before, the working fluids' a density difference does affect the separation performance in T-junction. Theoretically, the lesser dense fluid will tend to divert to the side arm while the denser fluid will tend to remain at the main and run arms. In a nutshell, it is proven that the larger the density differences of working fluids, more oil will tend to divert to the side arm and results in greater fraction of oil taken off.

Besides that, it is observed that the geometrical configuration also plays a role in phase separation, as discussed before the length ratio of pipe is identified as third factors most affecting the fraction of oil taken off. It would be interesting to investigate different configurations of T-junction to determine the best selection criteria for a much wider

range of flow conditions. Therefore, future work can be done to study the effect of inclination angle of both main arm and side arm. Other than that, the orientation of T-junction also should be considered for future research in order to achieve the desired separation targets such as the vertical main arm with horizontal side arm. Apart from that, the radius curvature between main and side arm also should be considered in future research. Lastly, more studies should be concentrated on the temperature effect on two phase separation efficiency in order to achieve more accurate result.

REFERENCES

[1] Azzopardi B.J., Whalley P.B. (1982, October). The effect of flow pattern on two phase flow in a T junction. *International Journal of Multiphase Flow*, **8**(5), 491-507.

[2] Pandey S., Gupta A., Chakrabarati D.P., Das G., Ray S. (2006, October). Liquid-liquid two phase flow through a horizontal T-junction. *Chemical Engineering Research & Design*, **84**(10), 895-904.

[3] Yang L., Azzopardi B.J., Belghazi A., (2005, January). Phase separation of liquid-liquid two phase flow at a T-junction. *AIChE Journal*, **52**(1), 141-149 .

[4] Wang L.Y., Wu Y.X., Zheng Z.C. et al. (2008, April). Oil-water two phase flow inside T-junction. *Journal of Hydrodynamics, Ser. B*, **20**(2), 147-153.

[5] Wren E. (2001). The simple T-junction & two phase flow. *Geometric effects on phase split at a large diameter T-junction*, 14-18.

[6] Abduvayt P., Manabe R., Watanabe T. et al. (2006, February). Analysis of oil/water flow tests in horizontal, hilly terrain and vertical pipes. *SPE Production & Operations*, **21**(1), 123-133.

[7] Flores J.G., Chen X.T., Sarica C. et al. (1999, May). Characterization of oil-water flow patterns in vertical and deviated wells. *SPE Production and Facilities*,**14**(2), 94-101.

[8] Pereyra E., Mohan R., Shoham O. (2013, June). A simplified mechanistic model for an oil/water horizontal pipe separator. *Oil and Gas Facilities,* **2**(3), 40-46.

[9] Brauner N. (n.d.).General description of liquid-liquid flows: Flow patterns. *Modelling & Control of Two-Phase Flow Systems*,1-5.

[10] Nadler M., Mewes O. (1997, February). Flow induced emulsification in the flow of two immiscible liquids in horizontal pipes. *Int. J. Multiphase Flow*, **23**(1), 56-68.

[11] Atmaca S., Sarica C., Zhang H.Q., Al-Sarkhi A.S., (2008). *Characteristic of oil/water flows in inclined pipes*, 41-46.

[12] Amirachakaran S., Oglesby K.D. (1989). Malinowsky M.S. et al. An analysis of oil/water flow phenomena in horizontal pipes. *In SPE production Operations Symposium, 13-14 March 1989, Oklohama City, Oklohama.*

[13] Trallero J.L., Sarica C., Brill J.P. (1997, August). A study of oil/water flow patterns in horizontal pipes. *SPE Production & Facilities*,**12**(3), 165-172.

[14] Azzopardi B. J., & Rea S. (2000, October). Phase separation using a simple T-junction. *In SPE Annual Technical Conference and Exhibition.*

[15] Vuong D.H., Zhang H.Q., Sarica C. et al. (2012, March). *Modeling high-viscosity oil/water occurent flows in horizontal and vertical pipes*. **17**(1), 243-250.

[16] Stenmark E. (2013, September). Multiphase flow theory: Modeling approaches. In *On Multiphase Flow Models in ANSYS CFD Software*. 4-6.

[17] Chen J. L., He L. M., Luo X. M. et al. (2012, June). Simulation of oil-water two phase flow and separation behaviors in combined t-junctions. *In Journal of Hydrodynamics*. **24**(6), 848-857.

[18] Huang S. (2005, October). Numerical simulation of oil-water hydrocyclone using Reynolds-stress model for eulerian multiphase flows. *In The Canadian Journal of Chemical Engineering*. **83**, 829-834.

[19] Al-Yaari M. A., & Abu-Sharkh B. F. (2011, November). CFD prediction of oil-water phase separation in 180° bend. *In Journal of Asian Transaction on Engineering*. **1**(5), 63-67.

[20] Frank T. H., Adlakha M., Lifante C et al. (n.d). Simulation of turbulent and thermal mixing in t-junctions using urans and scale-resolving turbulence models in ansys CFX. 1-23.

[21] Kanarachos S., & Flouros M. (n.d.). Simulation of the air-oil mixture flow in the scavenge pipe of an aero engine. *In Journal of Advances in Remote Sensing, Finite Differences and Information Security*.